IAEA-F1-CN-TH3/7

THEORY FOR ANGULAR MOMENTUM GENERATION AND THE PROBLEM OF POLOIDAL ROTATION *

B. COPPI, G. PENN, L.E. SUGIYAMA
Massachusetts Institute of Technology
Cambridge MA
United States of America

Abstract

THEORY FOR ANGULAR MOMENTUM GENERATION AND THE PROBLEM OF POLOIDAL ROTATION.

Results of the investigation of two basic problems involving the rotation of magnetically confined plasmas are presented. In the toroidal direction, significant plasma rotation has been produced in plasmas subject to ion cyclotron RF heating, in the absence of any evident direct angular momentum source. The theoretical model proposes the excitation of two classes of intrinsic magnetosonic whistler-like modes. The first, "contained" modes, has toroidal momentum in the same direction as that of the plasma current and is radially localized in the outer region of the plasma column, $r > 0.4a$. The other class is nonlocal and convects radially outwards, carrying the angular momentum in the counter-current direction to particles near the edge of the plasma column that are then scattered out of the plasma. Thus, rotation of the central part of the plasma column can be induced, with a velocity radial profile that is consistent with the anomalous transport of angular momentum resulting from the additional excitation of velocity-gradient-driven modes. The question of poloidal rotation and the evolution of poloidal flows in a torus is also examined. Results from the numerical simulation of MHD and two-fluid plasmas shows that compressional and other effects are important in the plasma response to rotation and provide an effective mechanism for damping poloidal flows in a torus on relatively fast time scales. The two-fluid response to rotation can be different than in MHD, due to differences in the symmetries of the equations, but they experience similar break-up of the poloidal rotation.

1. TOROIDAL ANGULAR MOMENTUM GENERATION

1.1. Symmetry breaking internal modes and generation of toroidal torque

We consider the process for the generation of torque on a plasma from balanced ICRF inputs[1, 2] to be related to the existence of a special class of magnetosonic-whistler modes at frequencies of the order of the ion cyclotron frequency and above, that can be excited by the injected waves. This class of modes is characterized by a strong asymmetry in the direction of poloidal propagation in that there are two types of modes, one convective and one standing. The contained modes, which propagate around magnetic flux surfaces but form standing modes in the radial direction, can be confined within a narrow radial layer located in the outer region of the plasma column[3]. For a realistic range of plasma parameters, including those of the Alcator C-Mod experiments, only modes with a poloidal phase velocity in the ion cyclotron direction are radially confined. This fixes the sign of their poloidal mode number m.

Radially confined modes can deposit their angular momentum on the plasma background as they damp against the plasma. In contrast, modes having the opposite phase velocity convect outward toward the edge of the plasma column, scattering particles that have angular momentum in the counter-current direction. In turn, these particles can lose their angular momentum to the outer viscous layer of the plasma column. When the current is increased, these particles are better confined and the rate of loss of angular momentum to the outer region decreases.

*Supported in part by the U.S. Department of Energy.

This is consistent with the experimental observation in the Alcator C-Mod experiment, that the induced plasma rotation diminishes as the plasma current is increased.

It is difficult to find contained modes that propagate primarily along the magnetic field (i.e., with large $k_{||}$) in the range of parameters that characterize the experiments. For modes propagating nearly perpendicular to field, the direction of the toroidal phase velocity is correlated with that of the poloidal phase velocity due to the magnetic field geometry, through the condition $n^0 \simeq m/q$. Here q is the inverse rotational transform, which in the limit of a cylindrical plasma is given by $q = rB_\zeta/R_0B_\theta$. The resulting net torque applied to the plasma is in the direction of the plasma current, consistent with experimental observations. Through the sign of q, the toroidal mode number for these modes changes sign if the current is reversed. The analysis therefore focuses on modes with nearly perpendicular propagation, $k_{||}^2 \propto (1 - n^0q/m)^2 \ll 1$.

To display the different features of contained modes from those of the unconfined magnetosonic-whistler waves, we consider the form of the effective potential V_{eff} for the two different types of modes. The radial eigenfunction of the standing modes is given by the equation

$$\frac{d^2\tilde{B}_{||}}{dr^2} - V_{\text{eff}}(r,\omega)\tilde{B}_{||} \simeq 0 \tag{1}$$

where

$$V_{\text{eff}} \simeq -\frac{\omega^2}{v_A^2 + k_{||}^2 D_H^2} - \frac{k_\perp \omega}{r(v_A^2 + k_{||}^2 D_H^2)} \frac{d}{dr}(D_H) + k_\perp^2, \tag{2}$$

v_A is the Alfvén velocity, and $D_H = B/\mu_0 ne$. The wave vector components $k_{||}$ and $k_\perp$ can be approximated as $k_\perp \simeq k_\theta = -m/r$ and $k_{||} \simeq -(m/Rq)(1 - n^0q/m)$, where m and n^0 are the poloidal and toroidal mode numbers, respectively.

The contained mode frequency, if positive, is roughly $\omega \simeq |k_\perp|v_A = |m|v_A/r_0$, where r_0 is the mode localization radius. For typical experimental parameters contained modes exist only for m positive; the poloidal phase velocity is in the ion cyclotron direction. If we consider the "quasi-flute" limit where $(1 - n^0q/m)^2 \ll 1$ and $k_{||}^2 D_H^2 \ll v_A^2$, that is $k_{||}^2 d_i^2 \ll 1$ where $d_i \equiv c/\omega_{pi}$, the modes are found to be clustered around a nearly unique radial surface $r = r_0$ which is determined by the density profile and the parameter d_i/a, a being the radius of the plasma column.

For plasma parameters typical of the Alcator C-Mod machine[4], $r_0 \simeq 0.7a$. In Fig. 1a the effective potential is shown for the two cases $m = 6$, $n^0 = 3$ and $m = -6$, $n^0 = -3$. The corresponding frequencies are 2.03 Ω_i and 1.66 Ω_i, respectively.

Thus for quasi-flute modes $n^0 \simeq m/q(r_0)$ and the propagation along $\hat{e}_\zeta$ is correlated in sign to that in the poloidal direction. There are also modes with $n^0/m > 0$ that are not of the flute type, in the sense that $|1 - n^0q/m| \gtrsim 1$, and modes with $n^0/m < 0$ that are never of the flute type. For sufficiently high frequencies, non-flute modes are excluded from only a relatively small region close to the plasma core. In the low frequency regime, quasi-flute modes, which have a distinctive dependence of their radial eigenmodes on the component of propagation parallel to the equilibrium magnetic field, are easier to excite.

The origin of the asymmetry in poloidal propagation is the Hall term in the Ohm's law, $\vec{E} + \vec{u}_i \times \vec{B} = \vec{J} \times \vec{B}/en$. As shown in Ref. [3], significant propagation along the equilibrium magnetic field tends to reduce the asymmetry between modes with opposite phase velocities and reduces the importance of the Hall effect in shaping the mode solutions. As a result, the asymmetry in the radial mode structure with respect to the direction of the poloidal phase velocity is greatest for modes which propagate nearly perpendicular to the equilibrium magnetic field.

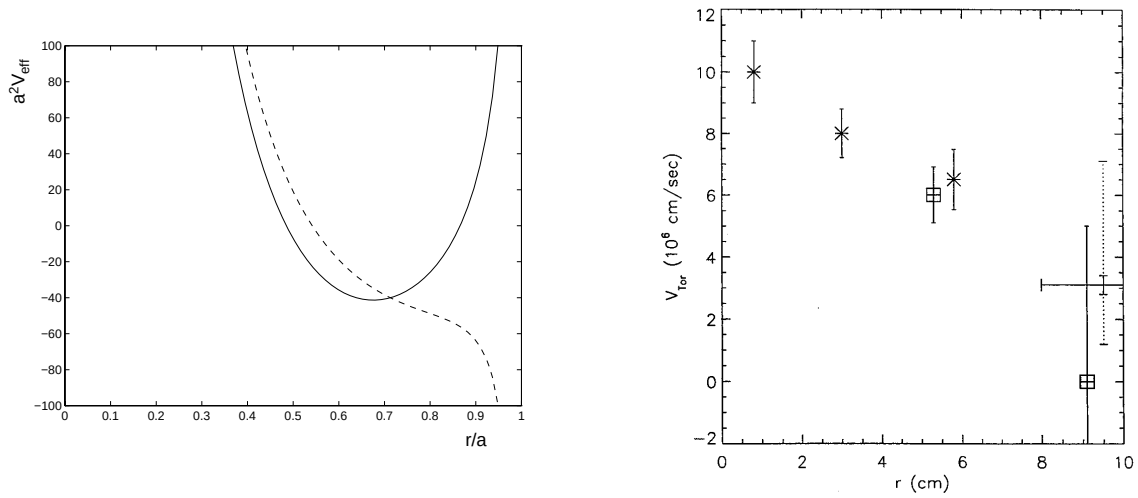

FIG. 1. a) Effective potential $V_{\rm eff}$ for modes propagating in the ion cyclotron ($m > 0$, solid line) and electron cyclotron directions ($m < 0$, dashed line). b) Radial profile of the toroidal velocity in the Alcator C-Mod experiments, from [2].

1.2. Angular momentum generation and transport

Let $\mathcal{E}$ be the RF energy acquired by the contained modes. Then we can argue that these modes will have toroidal angular momentum

$$\mathcal{L}_\zeta \simeq \mathcal{E} n^0/\omega, \tag{3}$$

where n^0 is the toroidal mode number and the frequency is roughly $\omega \simeq |k_\perp| v_A = |m| v_A/r_0$, with $n^0 \simeq m/q$. For the plasma parameters of the Alcator C-Mod experiments, contained modes exist only for $m > 0$, so that the poloidal phase velocity is in the ion cyclotron direction. The toroidal phase velocity is in the same direction as the equilibrium toroidal current. For positive q, $B_\zeta/B_\theta > 0$, this is also the direction of the toroidal field.

For a given toroidal velocity profile $v_\zeta(r)$, the plasma angular momentum is $\mathcal{L}_\zeta^P = V R_0 m_i \langle n_i v_\zeta \rangle$, where $\langle\ \rangle$ denotes a volume average, R_0 is the major radius, and V the plasma volume. Characteristic parameters for the Alcator C-Mod experiments are $a \simeq 0.22$ m, $R_0 \simeq 0.67$ m, $n_0 \simeq 10^{20}$ m^{-3}, $B_0 \simeq 5.3$ T, and $q(r_0) \simeq 2$, where the radius of localization is $r_0 \simeq 0.7\ a$. The ellipticity is $\kappa \lesssim 1.8$. During ICRF heating, the core density increases up to 2.5×10^{20} m^{-3}. For a deuterium plasma, the Alfvén velocity is $v_A \simeq 8200$ km/s. The peak plasma temperature is about 2 keV and the deuterium thermal velocity is about 450 km/s. For a peak rotation velocity of 100 km/s, excluding the diamagnetic velocity contribution, with a sharply peaked velocity profile as shown in Fig. 1b, the angular momentum is estimated to be $\mathcal{L}_\zeta^P \simeq \alpha_\mathcal{L} 10^{-3}$ J-s, where $\alpha_\mathcal{L} \lesssim 1$.

The loss rate of angular momentum is then $\mathcal{L}_\zeta^P/\tau_\mathcal{L} \simeq \alpha_\mathcal{L} 10^{-2} (10^{-1}/\tau_\mathcal{L})$ J where $\tau_\mathcal{L}$ is the angular momentum loss time. On the other hand, the rate of supply of angular momentum to contained modes can be estimated as $\epsilon_W P_W/(q v_A/r_0)$, where P_W is the total ICRF power and ϵ_W is a small parameter. Therefore for $P_W \simeq 2$ MW, this quantity is about $2\epsilon_W$ J and we can see that ϵ_W can be adequately small.

The transport of angular momentum is observed to be anomalous. Furthermore, induced rotation is seen only in regimes where the anomalous ion thermal energy transport is depressed. Thus we argue that when ion temperature gradient driven modes are strongly excited, for example before the H-mode regime is established, the flux of angular momentum is given by

$$, _J \simeq -D_i^{\rm th} \left[\frac{dJ}{dr} + \frac{dT_i}{dr} \frac{R_o n}{v_w} \right], \tag{4}$$

where J is the angular momentum density, $D_i^{\rm th}$ the effective diffusion coefficient produced by ion temperature gradient driven modes that also carry angular momentum outwards [5], and v_w is a characteristic wave velocity. When the ion thermal transport is large, the angular momentum that is deposited in the outer region of the plasma column does not induce significant plasma rotation. In contrast, when a thermal transport barrier forms, as in the case of the H-mode regime, a net radial influx of angular momentum is produced at the edge of the region that is not affected by contained modes. In the absence of outward transport, unrealistically peaked profiles of J would develop. It is therefore reasonable to assume that velocity gradient driven modes are excited. If the gradient of J is limited by the effects of such modes, then

$$-Jv_J - D_J\frac{dJ}{dr} \simeq 0, \tag{5}$$

where the term proportional to D_J indicates the transport of angular momentum resulting from the velocity gradient driven modes. Here, v_J vanishes at $r = 0$ and is finite at $r = r_Q$, the edge of the quiescent region that is unaffected by contained modes. Thus Eq. (5) can produce the desired profiles.

1.3. Experimental observations

Toroidal rotation induced by balanced ICRF heating has been observed in experiments carried out by the Alcator C-Mod machine [2]. There $v_{i\zeta}$ for the deuteron species may be estimated as

$$E_r - \frac{1}{c}v_{i\zeta}B_\theta - \frac{T_i}{n_i e}\frac{dn_i}{dr} - \epsilon_T\frac{1}{e}\frac{dT_i}{dr} \simeq 0, \tag{6}$$

where $\epsilon_T \ll 1$, recognizing that the component $n_i dT_i/dr$ of the pressure gradient is nearly compensated by a poloidal velocity, according to neoclassical transport theory. The impurity (argon) poloidal velocity $v_{I\theta}$ was found to be below the threshold of observation. Thus we can argue that the bulk ion diamagnetic velocity contributed considerably less than half of the toroidal flow velocity.

Similar experiments have been performed on the JET machine[1], and observations of induced rotation in the direction of the plasma current were attributed to the diamagnetic velocity. The radial profile of the velocities was not measured, but the line average of the fluid flow at 20–30 cm below the magnetic axis indicated a toroidal velocity of up to 50 km/s. During ICRH and while H-mode confinement was maintained, the toroidal flow of the plasma accelerated at a uniform rate of 15 km/s^2. The plasma parameters for these experiments were $a \simeq 0.95$ m, $R_0 \simeq 2.95$ m, $B_0 \simeq 2.8$ T, $I \simeq 3$ MA and $Z_{eff} \simeq 2.5$.

Finally, we point out that direct experimental evidence for the existence of contained modes produced by an injected population of high energy particles appears to have been provided recently by the START machine[6].

2. POLOIDAL ROTATION

Radial electric fields are also associated with plasma rotation in the poloidal direction. Due to the lack of symmetry in this direction, detailed theoretical understanding is difficult. Nevertheless, both theory and experiment indicate that poloidal rotation is directly related to fundamental questions of plasma confinement [7][8]. Analyses carried out so far, e.g., [9][10][11], have neglected the full effects of compressibility and toroidal geometry, by using aspect ratio expansion and a local approximation in the radial coordinate. The present study considers the behavior of fluid models, using the the 3D, toroidal initial value code, MH3D-T [12], and finds that these factors are significant.

Only strict toroidal axisymmetry is considered here, as a first approximation. The time scales of interest are shorter than the collisional ones on which damping is to be expected

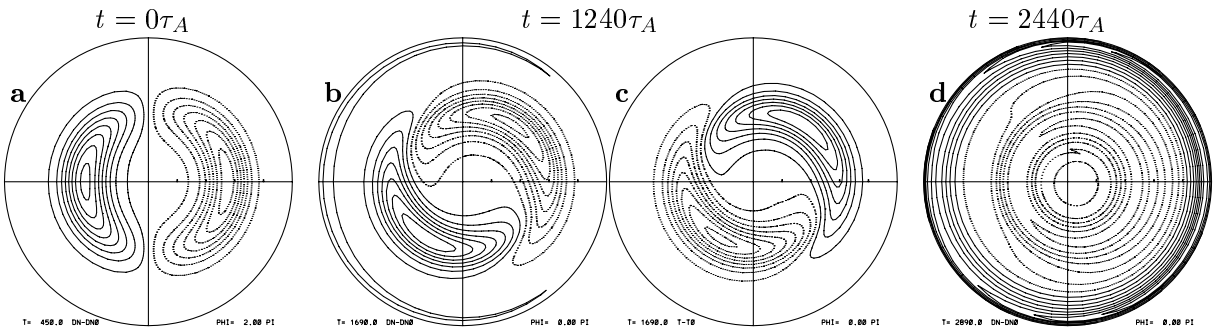

FIG. 2. Formation of a stationary poloidally asymmetric density perturbation in an MHD torus with $R/a = 20$, a) Initial $m = 1$ density perturbation, $\delta n/n \lesssim 0.1$, with a small $v_\theta(\psi) > 0$ (counterclockwise) motion applied to a stationary equilibrium. Equally spaced contours in a vertical cross section, with positive values are solid lines, negative dashed. The axis of symmetry is to the left. b) Density and c) temperature perturbations balance in the first steady state, as $|\mathbf{v}| \to 0$. Apparent poloidal motion of the density blob ceases by $\sim 440\tau_A$, but v_θ continues to decay. After a thermal $\kappa_\parallel$ is applied to this state, the d) density and temperature (similar contours, not shown) nearly return to the original symmetric state, $|\delta n/n| < 0.004$ relative to the initial equilibrium, $|\delta T/T|$ smaller.

(e.g., ion viscosity and neoclassical effects). Some effects of resistivity are considered, since it is intimately connected to fluid rotation [13].

2.1. Equilibrium

The basic picture of rotational equilibrium and stability in a torus is as follows. An ideal MHD equilibrium exists with temperature T, $I = RB_\zeta$, and electrostatic potential ζ as functions of flux ψ, for special velocity profiles $\mathbf{v} = (K(\psi)/n)\mathbf{B} + R\Omega(\psi)\hat{\zeta}$, where K and Ω are arbitrary functions of flux. Resistivity allows Pfirsch-Schlüter convective cells with a flow toward the outside of the torus along the midplane and an associated, enhanced density radial outflow. Resistivity also causes an acceleration of existing poloidal plasma motion [13], up to a limiting value related to the diamagnetic or sound speeds, depending on the plasma model used, unless damped by viscosity or other dissipation. In practice, these processes are found to be strongly affected by compressional and other effects, not usually included in the theoretical analysis.

When the plasma evolves from a poloidally rotating state, the plasma density and the (ion) temperature can remain as poloidally asymmetric functions of space as the poloidal velocity goes to zero, particularly at large aspect ratio. The asymmetries may then decay on longer, collisional time scales. Steady state in MHD (without neoclassical effects) requires that the pressure be a function of flux, which implies that the density and temperature perturbations must balance. Poloidally asymmetric densities and ion temperatures can still occur when the electron temperature is assumed to remain close to a flux function, due to the rapid electron thermal equilibration along the magnetic field lines.

In a simple flux-averaged surface picture, which neglects most radial effects, poloidal plasma flows are directly related to poloidally asymmetric variations of the plasma density, which act as both response and drive [11]. The unstable density perturbations are basically $m = 1$ and unbalanced across the horizontal midplane. Figure 2 illustrates a poloidally asymmetric steady state resulting from an initial $m = 1$ density perturbation and a small poloidal velocity, for $R/a = 20$. Applying a large thermal $\kappa_\parallel$ that rapidly equalizes the temperature on a flux surface then causes the asymmetric stationary state to evolve to a second stationary state with poloidal symmetry, close to the original state, after passing through a transient rotating phase.

In most cases of interest, only T_e has a rapid isotropization along the magnetic field lines. Considering the explicit thermal conductivity to represent the part that operates in addition to the sound and Alfvén wave effects that are always present in the fluid equations, the two-fluid results show that nonzero electron $\kappa_{\parallel e}$ with ion $\kappa_{\parallel i} = 0$ is closer to the MHD case with total

$\kappa_{||} = 0$ than to $\kappa_{||} \sim \kappa_{||e}$, for time scales shorter than the ion-ion collision time. Thus the MHD-consistent assumption that the total temperature $T \equiv p/n$ remain close to a flux function gives an artificially strong constraint on the pressure.

A further equilibrium result is that the resistively driven radial density outflow in a torus, the sum of the classical and Pfirsh-Schlüter flows, can reverse to a density inflow under paramagnetic conditions, i.e., when the induced poloidal J_θ is positive so that its contribution to the equilibrium radial pressure gradient, $\mathbf{J} \times \mathbf{B} = \nabla p$ is positive, $J_\theta \times B_\zeta > 0$ (the toroidal current, whose contribution $J_\zeta \times \mathbf{B}_\theta$ is always negative, is balanced by an applied toroidal electric field $E_\zeta = \eta_{||} J_\zeta$ and does not contribute to radial flow). A large positive J_θ, for example, occurs in high field experiments. The neoclassical PS diffusion enhancement is proportional to the pressure gradient contribution from J_θ. A density inflow is readily demonstrated by MHD and two-fluid simulation at low beta. It is accompanied by a similar temperature inflow. The inflow is continuous and must be balanced by an anomalous outward diffusion in equilibrium. In practice, the radial diffusion due to realistic collisional resistivities is small, except perhaps near the plasma edge.

2.2. Toroidal equilibrium flows

Tests of the MHD steady state with applied toroidal or parallel flows show that impulses of toroidal momentum are subject to compressional effects that require dissipation to suppress. In general, oscillations in the perpendicular ($\perp \zeta$) velocity are triggered, which rapidly degenerate into fine scales unless they are damped by sufficiently strong dissipatiion (η, $\kappa_\perp$, etc.) Applying a velocity perturbation v_ζ or $v||$ of the expected steady state functional form to a stationary MHD equilibrium causes an outward (large R) shift of the plasma mass due to the centrifugal effects of the v_ζ motion. The reaction and compressional forces produced by the encounter with the fixed plasma boundary produces poloidal and radial velocity components, which begin to oscillate radially. The oscillations propagate radially outward over the rotating region. The orientation and convective cell structure are reminiscent of the $m = 1$ Pfirsh-Schlüter convective cells, but are more radially localized and oscillate in sign. (The oscillations of the poloidal v_θ are oriented vertically and those in v_ψ, related by $\mathbf{v}_{\perp\zeta} \simeq \nabla u \times \hat{\zeta}$, horizontally.) At small resistivity, they rapidly degenerate into small scales in space and time, on an MHD time scale. Only in the presence of sufficient dissipation, such as resistivity or perpendicular (thermal) diffusion, do the velocity oscillations remain macroscopic in scale and damp, leaving steady state plasma flows of the expected form. The oscillatory nature of transient poloidal and toroidal flows in a torus, due to compressional effects, is a characteristic feature.

2.3. Poloidal acceleration

While spontaneous resistive, "Stringer spin-up" acceleration of the poloidal plasma velocity exists [13][14], due to the typically small values of resistivity it is usually limited to the plasma edge and easily damped by viscosity and other dissipative processes. Simulation shows that compressional effects are even more effective in limiting spin-up, on MHD time scales. Typically, an unbalanced density perturbation rotates convectively around the outside of the torus until the positive density approaches the inboard side of the torus, where it stalls on the inboard midplane as the poloidal velocity reverses, and then gradually breaks up into smaller scales. This occurs even at relatively large aspect ratio, $R/a = 20$. At the smaller aspect ratios typical of experiments, the compressional component of the velocity can couple strongly to an $m = 2$ harmonic. An acceleration of the initial convective motion of the density with increasing resistivity can be demonstrated, but has little effect on the final result, since the motion of the density soon ceases to be convective. A qualitatively similar scenario is shown in Fig. 3.

A previous MHD numerical simulation clearly demonstrated resistive Stringer spin-up to near the sound speed [14]. In that case, however, the magnetic field was static, $\partial \mathbf{B}/\partial t = 0$. The simulation also saw the oscillatory effects of the magnetostatic geodesic acoustic mode [15]

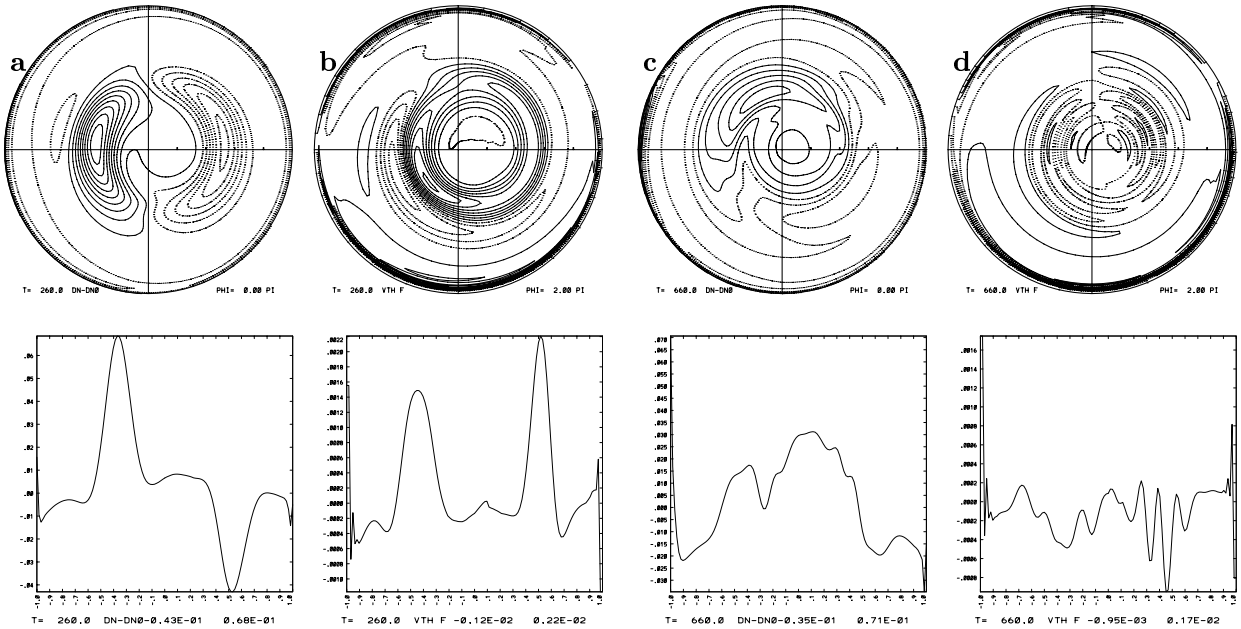

FIG. 3. Break-up and decay of poloidal rotation driven by density in two-fluids and smaller aspect ratio. Initial MHD equilibrium and density perturbation as in Fig. 2a, except $R/a = 4$ and initial $v_{i\theta} = 0$. a) Perturbed density and b) $v_{i\theta}$ contours and profiles at $t = 120\tau_A$, after initial transients disappear. Early rotation velocities are on the order of $|v_{i\theta}| \sim |v_{*i}|$. c) and d) Same at $t = 520\tau_A$, when coherent structure breaks up and rotation disappears. The lower frames show corresponding profiles, the right half along $\theta = 0$, the outer (right) midplane, and the left half along $\theta = \pi/2$, the upper vertical axis.

due to the $\tilde{E}_r \times B_\zeta$ velocity. In the non-magnetostatic case, this mode is often overshadowed by oscillations associated with the compressional term in the velocity.

2.4. Fluid equation symmetries

A two-fluid model includes the ion gyroviscous stress tensor, the Hall term and electron pressure gradient in Ohm's law. Separate density and temperature evolution and different ion and electron parallel thermal conductivities are allowed. For the poloidal rotation problem, some differences from MHD depend solely on the magnitude of the diamagnetic drifts relative to the applied rotation. Others depend on the breaking of the symmetry of the MHD equations in (θ, ζ), in a toroidal geometry. Simulation results generally confirm that the two-fluid steady state has ion fluid velocity $v_{i\theta} = 0$, in agreement with [9].

In toroidal geometry, the MHD system of equations preserves certain symmetries in the dependence of the fundamental MHD variables on the two natural angles, in the sense that each scalar variable has a single well-defined sign, in the relation $f(\theta, \zeta) = \pm f(-\theta, -\zeta)$. A nonrotating MHD equilibrium, and also typical MHD normal mode perturbations of that equilibrium, has a specific set of signs that defines the symmetry of the system. For example, in equilibrium and for a typical reconnecting mode, the poloidal magnetic flux ψ has a plus sign, while the velcity stream function u has a negative sign. Toroidal rotation breaks this symmetry, since the globally rotating part of v_ζ has positive symmetry, but typical perturbations from a stationary MHD equilibrium would have negative symmetry. For a toroidally axisymmetric equilibrium this symmetry breaking makes no difference, since $\partial/\partial\zeta = 0$. For poloidal rotation, however, the opposite symmetry terms are significant.

The major two fluid terms all have opposite symmetry from the MHD terms to which they add, so that the symmetry-preserving properties of the equations are broken. This makes certain marginally stable MHD perturbations, which would be stationary in the absence of an initial applied velocity 'kick' in MHD, naturally rotating in two-fluids. An important potential

example is a poloidally asymmetric density perturbation that is symmetric about the horizontal midplane, which describes the results of pellet injection along the midplane. Such a density accumulation has a natural poloidal rotation in two-fluids. In practice, the importance of the rotation depends on the relative time scales for pellet ablation and parallel symmetrization, compared to the local diamagnetic velocities.

As an example, the density perturbation case of Fig. 3. is repeated for two-fluids at smaller aspect ratio, $R/a = 4$. Here the initial condition on the poloidal velocity is zero applied rotation, $v_{i\theta} = 0$. The equilibrium $T_e = T_i$, with a nonzero electron thermal conductivity $\kappa_{\|e}$, but ion $\kappa_{\|i} = 0$. A stationary nonrotating state is now approached by the breaking up of the coherent density and poloidal rotation structure rather than by balancing δn and δT_i. In two-fluids, the main density perturbation spontaneously moves off the midplane and, at smaller aspect ratio, makes a primarily non-convective poloidal excursion around the magnetic axis, as a compressional $m = 2$ mode is excited (not shown), before settling back near the starting point on the inboard midplane. It gradually breaks up radially and the poloidal velocity develops radial oscillations and decays in magnitude (Fig. 3d). This type of decay is typical when random initial density perturbations or poloidal rotation profiles are applied, in two-fluids and MHD.

REFERENCES

[1] ERIKSSON, L.-G., RIGHI, E., ZASTROW, K.-D., Plasma Phys. Cont. Fusion, **39** (1997) 27.

[2] RICE, J.E., et al., Nucl. Fusion, **38** (1998) 75.

[3] COPPI, B., PENN, G., RICONDA, C., Ann. Phys., **261** (1997) 117.

[4] HUTCHINSON, I.H., et al., Phys. Plasmas, **1** (1994) 1511.

[5] COPPI, B., Plasma Phys. Contr. Fusion, **36B** (1994) 107.

[6] MCCLEMENTS, K.G., et al., To be published in Proc. of the 1998 Varenna Symposium on Plasma Theory, Varenna, Italy.

[7] BURRELL, K.H., Phys. Plasmas **4** (1997) 1499.

[8] ROSENBLUTH, M.N., HINTON, F.L., Phys. Rev. Lett., **80** (1998) 724.

[9] BOWERS, E., WINSOR, N.K., Phys. Fluids **14** (1971) 2203.

[10] HASSAM, A.B., KULSRUD, R.M. Phys. Fluids **22** (1979) 2097.

[11] HASSAM, A.B., and DRAKE, J.F., Phys. Fluids B **5** (1993) 4022.

[12] PARK, W., et al., Proc. 16th Int'l. IAEA Conf. on Fusion Energy, Montreal, 1996 (I.A.E.A., Vienna, 1997) Vol. 2, p. 411.

[13] STRINGER, T.E., Phys. Rev. Lett **22** (1969) 1770.

[14] WINSOR, N.K., JOHNSON, J.L., DAWSON, J.M., J. Comput. Phys. **6** (1970) 430; GREENE, J.M., et al., Phys. Fluids **14** (1971) 1258.

[15] WINSOR, N.K., JOHNSON, J.L., DAWSON, J.M., *Phys. Fluids* **11** (1968) 2448.